UC San Diego

UC San Diego Previously Published Works

Title

A Novel, Direct NO Donor Regulates Osteoblast and Osteoclast Functions and Increases Bone Mass in Ovariectomized Mice

Permalink

https://escholarship.org/uc/item/6j07m9nn

Journal

Journal of Bone and Mineral Research, 32(1)

ISSN

0884-0431

Authors

Kalyanaraman, Hema
Ramdani, Ghania
Joshua, Jisha
et al.

Publication Date

2017

DOI

10.1002/jbmr.2909

Peer reviewed

eScholarship.org Powered by the California Digital Library
University of California

Author Manuscript

Author Manuscript

Author Manuscript

Author Manuscript

HHS Public Access

Author manuscript

J Bone Miner Res. Author manuscript; available in PMC 2018 January 01.

Published in final edited form as:

J Bone Miner Res. 2017 January ; 32(1): 46–59. doi:10.1002/jbmr.2909.

A NOVEL, DIRECT NO DONOR REGULATES OSTEOBLAST AND OSTEOCLAST FUNCTIONS AND INCREASES BONE MASS IN OVARIECTOMIZED MICE

Hema Kalyanaraman[1], **Ghania Ramdani**[1], **Jisha Joshua**[1], **Nadine Schall**[3], **Gerry R. Boss**[1], **Esther Cory**[2], **Robert L. Sah**[2], **Darren E. Casteel**[1], and **Renate B. Pilz**[1,4]

[1]Department of Medicine, University of California, San Diego, La Jolla, CA 92093-0652

[2]Department of Bioengineering, University of California, San Diego, La Jolla, CA 92093-0652

[3]Institute of Pharmacology and Toxicology, University of Bonn, 53105 Bonn, Germany

Abstract

Most FDA-approved treatments for osteoporosis target osteoclastic bone resorption. Only PTH derivatives improve bone formation, but they have drawbacks, and novel bone-anabolic agents are needed. Nitrates, which generate NO, improved BMD in estrogen-deficient rats and may improve bone formation markers and BMD in post-menopausal women. However, nitrates are limited by induction of oxidative stress and development of tolerance, and may increase cardiovascular mortality after long-term use. Here we studied nitrosyl-cobinamide (NO-Cbi), a novel, direct NO-releasing agent, in a mouse model of estrogen deficiency-induced osteoporosis. In murine primary osteoblasts, NO-Cbi increased intracellular cGMP, Wnt/β-catenin signaling, proliferation, and osteoblastic gene expression, and protected cells from apoptosis. Correspondingly, in intact and ovariectomized (OVX) female C57Bl/6 mice, NO-Cbi increased serum cGMP concentrations, bone formation, and osteoblastic gene expression, and in OVX mice, it prevented osteocyte apoptosis. NO-Cbi reduced osteoclasts in intact mice and prevented the known increase in osteoclasts in OVX mice, partially through a reduction in the RANKL/osteoprotegerin gene expression ratio, which regulates osteoclast differentiation, and partially through direct inhibition of osteoclast differentiation, observed *in vitro* in the presence of excess RANKL. The positive NO effects in osteoblasts were mediated by cGMP/PKG, but some of the osteoclast-inhibitory effects appeared to be cGMP-independent. NO-Cbi increased trabecular bone mass in both intact and OVX mice, consistent with its *in vitro* effects on osteoblasts and osteoclasts. NO-Cbi is a novel direct NO-releasing agent that, in contrast to nitrates, does not generate oxygen radicals, and combines anabolic and anti-resorptive effects in bone, making it an excellent candidate for treating osteoporosis.

[4]Corresponding Author (to whom reprint requests should be addressed): Renate B. Pilz, rpilz@ucsd.edu, University of California, San Diego, 9500 Gilman Dr., La Jolla, CA 92093-0652. Phone: 858-534-8805, Fax: 858-534-1421.

Disclosures: None of the authors have any conflicts of interest to declare.

Supplemental Data are included with this submission.

Author Manuscript Author Manuscript Author Manuscript Author Manuscript

Keywords

Osteoporosis; Preclinical Studies; Anabolics; Molecular Pathways-Remodeling

INTRODUCTION

Bone undergoes constant remodeling, with osteoclasts resorbing bone, and osteoblasts generating new bone by secreting matrix and becoming entombed in the calcified matrix as osteocytes.[1, 2] Osteoblast differentiation from bone marrow stromal cells is under control of multiple factors, including Wnt family proteins.[1, 2] Cells of osteoblastic lineage produce RANKL and its decoy receptor osteoprotegerin (OPG); the ratio of the two proteins controls osteoclast differentiation from monocytes.[1, 2] Imbalanced bone remodeling leads to osteoporosis, a highly prevalent and serious public health concern, with osteoporosis-associated fragility fractures causing significant morbidity, mortality, and economic cost.[2–4] Current osteoporosis therapies primarily reduce bone resorption; however, these agents secondarily reduce bone formation and cause rare, potentially serious side effects.[2, 3, 5] PTH preparations are the only currently FDA-approved drugs that stimulate bone formation, but they also enhance resorption, their anabolic effect wanes over time, and their use is limited to two years, due to osteosarcoma development in rats.[2, 5, 6] Although post-menopausal estrogen deficiency is a major cause of osteoporosis, estrogen replacement is no longer recommended for osteoporosis prophylaxis or treatment, because breast cancer and thromboembolic risks outweigh the skeletal benefits.[2, 5, 7] Fear of complications explains, in part, why less than one-fifth of osteoporotic women in the U.S. receive treatment, and treatment compliance is poor.[3, 8] Thus, new bone-anabolic agents are urgently needed that are safe for long-term use.

Estrogens restrain osteoclast differentiation and survival, while promoting survival of osteoblastic cells; thus, estrogen deficiency-induced bone loss is at least partially explained by increased osteoclastic bone resorption and apoptotic osteocyte loss.[9–12] Mechanical stimulation also enhances osteoblast and osteocyte survival while suppressing RANKL production, and decreased physical activity contributes to bone loss in the elderly.[10, 13] Both estrogen treatment and mechanical stimulation induce osteoblasts and osteocytes to produce the second messenger NO.[14, 15] NO activates soluble guanylate cyclase to generate cGMP, which in turn stimulates protein kinase G (PKG). We found that NO mediates the pro-survival effects of estrogens and mechanical stimulation in osteoblasts and osteocytes via cGMP/PKG signaling, with cytosolic PKG I and membrane-bound PKG II playing different, but complementary roles.[14–16] Studies in NO synthase (NOS)-deficient mice support an important role of NO in osteoblast and osteoclast biology, and treating mice with NOS inhibitors blocks the bone-protective effects of estrogen or mechanical stimulation.[17–19]

Organic nitrates generate NO *in vivo* after mitochondrial biotransformation; nitrates are used to treat coronary insufficiency and heart failure, and epidemiological studies suggest their use may reduce fracture risk.[20–22] Based on these data and preclinical studies showing a bone-protective effect of organic nitrates in OVX rats,[23, 24] several clinical trials examined the skeletal effects of organic nitrates in post-menopausal women. In two separate small

Author Manuscript Author Manuscript Author Manuscript Author Manuscript

studies, nitroglycerin prevented bone loss after ovariectomy, and isosorbide mononitrate improved BMD in post-menopausal women with established osteoporosis.[25, 26] However, a large, placebo-controlled trial showed no effect of transdermal nitroglycerin on BMD in post-menopausal women with osteopenia.[27]

Organic nitrates are the only NO donors currently FDA-approved for long-term use, but clinical benefits of organic nitrates are limited by development of tolerance and induction of oxidative stress.[28–31] Nitrates require enzymatic activation to release NO, and this reaction generates reactive oxygen species, especially O_2^-, which can have detrimental effects in the cardiovascular and skeletal systems.[10, 30, 32] Here, we examined the skeletal effects of a novel NO donor, nitrosyl-cobinamide (NO-Cbi), derived from the vitamin B_{12} precursor cobinamide; it releases NO directly, without biotransformation or generation of reactive oxygen species.[33–36] We found that NO-Cbi enhanced trabecular bone mass in intact and OVX mice by enhancing osteoblast activity and inhibiting osteoclast differentiation.

MATERIALS AND METHODS

Materials

Antibodies against Akt, Akt(pSer^{473}), Erk1(pTyr^{204}), GSK-3β, GSK-3β(pSer^{9}), and cleaved caspase-3 were from Cell Signaling, and antibodies against Erk1/2 and β-actin were from Santa Cruz Biotechnology. A β-catenin-specific antibody and fluorophore-labeled secondary antibodies were from InVitrogen. DETA-NONOate was from Cayman Chemicals, and the cGMP agonist 8-(4-chlorophenylthio)-cGMP (8-pCPT-cGMP) was from BioLog.

Preparation of NO-Cbi

NO-Cbi was generated by reducing dinitrocobinamide under deoxygenated conditions. Ascorbic acid and dinitrocobinamide were incubated under argon at a ratio of 5:1 for 1 h at RT; then the solution was purged with argon to remove any free NO. NO-Cbi was stable at RT for at least 1 month when filter-sterilized and stored under argon protected from light.

Animal Experiments

Ten week-old female C57Bl/6 mice were purchased from Jackson Laboratories. They were maintained in accordance with the “Guide for the Care and Use of Laboratory Animals” (2011, 8th ed., Washington, D.C., Natl. Research Council, Natl. Academies Press), and all experiments were approved by the Institutional Animal Care and Use Committee of the University of California, San Diego. Mice were housed at 3–4 animals per cage in a temperature-controlled environment with a 12 h light/dark cycle; they were fed standard Teklad Rodent Diet with ad lib access to food and water. After one week of acclimatization, mice weighing 19.5–22.0 g were randomly divided into three groups—Groups 1 and 2 (eight mice each) underwent bilateral ovariectomy, while Group 3 (six mice) underwent a sham operation. One mouse in Group 1 had to be euthanized post-operatively because of suture failure. Beginning one week post-surgery, mice received daily i.p. injections six days per week for five weeks, either vehicle (0.1 ml 9.25 mM ascorbic acid, Group 1), or NO-Cbi (10 mg/kg/d given as 0.1 ml of 1.85 mM NO-Cbi, Group 2). In a separate experiment, 12 week-old intact female mice (six mice per group) were randomized to receive either vehicle or

Author Manuscript Author Manuscript Author Manuscript Author Manuscript

NO-Cbi on the same dose and schedule for five weeks. This NO-Cbi dose did not significantly reduce systolic blood pressure (< 10 mm Hg), consistent with our previous report,[33] and the NO-Cbi-treated mice showed no signs of toxicity and had similar weight gain during the experiment as the corresponding vehicle-treated groups. Double calcein labeling was performed by intraperitoneal injection of calcein (25 mg/kg) at seven and four days before euthanasia. Mice were euthanized one hour after the last drug or vehicle injection by CO_2 intoxication and exsanguination; blood samples were collected by cardiac puncture and allowed to clot. Femoral and tibial bones were dissected for quantitative RT-PCR, histology, and micro-CT analyses.

Mice carrying floxed *prkg2* alleles (PRKG2$^{f/f}$ mice)

To generate PRKG2$^{f/f}$ mice, we PCR-amplified genomic DNA fragments encoding *prkg2* exon III with flanking sequences from 129/SvJ ES cells using KOD polymerase (EMD Millipore Corporation). The *prkg2*-floxed construct was assembled in the vector pDLNL (gift from Ju Chen of UCSD) and consisted of a 4.2 kb 5′ arm, a 0.55 kb fragment including exon III flanked by LoxP sites, a 1.3 kb *neo* cassette flanked by FRT sites, and a 3kb 3′ arm. All PCR products and fusion sites were sequenced. The construct was electroporated into R1 ES cells derived from 129/SvJ mice, and G418-resistant clones were isolated and screened by PCR; homologous recombination was confirmed by Southern blot analysis using probes outside of the 5′ and 3′ arms. A recombinant clone with normal chromosome analysis in 20 metaphase spreads was injected into C57Bl/6 blastocysts to establish germline chimeric mice. Heterozygous PRKG2$^{f/+}$ mice were mated with homozygous FLPeR mice containing FLPe recombinase (from Jackson Laboratories) to remove the *neo* cassette. PRKG2$^{f/+}$ mice were backcrossed for five generations into the C57Bl/6 background.

Culture of murine primary osteoblasts (POBs)

POBs were isolated from the femurs and tibiae of 8–12 week-old C57/Bl6 mice, and from PRKG2$^{f/f}$ mice in a mixed background or after backcrossing into the C57Bl/6 background (as indicated). POBs were grown in DMEM (25 mM glucose) supplemented with 10% FBS, as described.[16, 37] In some cases, ascorbate (0.3 mM) and β-glycerolphosphate (10 mM) were added to the medium to induce differentiation. Cells were used at passages 1–5, and were checked for mineralization capacity.[37] To delete exon III of PRKG2, cells from PRKG2$^{f/f}$ mice were infected with adenovirus encoding CRE recombinase (or control virus expressing β-galactosidase, LacZ) at an MOI of 30 and were used 48 h later.

Culture of murine primary osteoclasts

Osteoclasts were generated from murine bone marrow as described.[38] Briefly, bone marrow cells were plated at 10^6 cells/cm^2 in α-Minimal Essential Medium with 10% FBS and 50 ng/ml M-CSF, and non-adherent cells were discarded after 48 h. RANKL (150 ng/ml) was added on day 3, and medium was replaced on days 5 and 7; the indicated drugs were added with fresh medium on days 3, 5, and 7. On day 8, cultures were fixed and stained for TRAP using a commercially-available kit (Sigma), or were harvested for RNA isolation. To delete PRKG2, cells were infected 24 h after plating with CRE adenovirus (or control virus expressing green fluorescent protein, GFP) at an MOI of 10; medium was replaced 24 h later when RANKL was added, and cells were examined 5 d later.

Author Manuscript Author Manuscript Author Manuscript Author Manuscript

Quantitative RT-PCR assays

Frozen bone shafts (frozen at −80°C after removal of bone marrow cells) were pulverized with a mortar and pestle in liquid nitrogen. RNA was purified using Trizol-reagent (Molecular Research Center, Inc.) and 1 μg of RNA was reverse-transcribed and quantitative PCR was performed using a MX3005P real-time PCR detection system with Brilliant II SYBR® Green QPCR Master Mix (Agilent Technologies).[16] Primer sequences are described in Supplemental Table 1; all primers were tested with serial cDNA dilutions. Relative changes in mRNA expression were analyzed using the $2^{-\Delta\Delta Ct}$ method, with 18S rRNA serving as an internal reference; we used mean ΔCT values (gene of interest minus 18S rRNA) measured in the vehicle-treated control groups to calculate ΔΔCT values for the corresponding NO-Cbi-treated groups.

Preparation of bone cell extracts and Western blotting

Protein extracts were prepared from mouse bones as described previously.[37] Briefly, ~50 mg of pulverized bone was incubated for 15 min on ice in 50 mM Tris-HCl pH 8.0, 150 mM NaCl, 2 mM EDTA, 1% Triton X-100, 0.1% SDS, 0.5% sodium deoxycholate, 2 mM Na_3VO_4, 10 mM NaF, and protease inhibitor cocktail. The samples were centrifuged at 13,000 g for 15 min at 4°C. Supernatants were boiled in SDS sample buffer, and proteins were resolved by SDS-PAGE and analyzed by Western blotting as described.[14] Films were scanned using Image J software.

Quantitation of NOx and cGMP

NO production was measured based on nitrite and nitrate accumulation in the medium with a two-step colorimetric assay, as previously described.[14] Serum cGMP concentrations were measured by ELISA using a kit according to the manufacturer's protocol (Biomedical Technologies Inc., MA).

Proliferation Assay

POBs in 6-well dishes were cultured in 0.1% FBS overnight and treated with NO-Cbi for 1 h; cells were then transferred to fresh medium with 0.1% FBS and 10 μCi of [methyl-^{3}H]thymidine (20 Ci/mmol, final concentration 0.5 μM) for 24 h. Cells were extracted *in situ* in ice-cold 10% trichloroacetic acid, precipitated DNA was collected on glass microfiber filters, and radioactivity on washed filters was measured by scintillation counting.

Immunofluorescence Staining

POBs were plated on glass coverslips, transferred to medium containing 0.1% FBS or 0.1% BSA, and incubated in the absence or presence of NO-Cbi for the indicated time. Cells were fixed and permeabilized and incubated with cleaved caspase-3- or β-catenin-specific antibodies (both at 1:100 dilution), followed by secondary antibodies conjugated to FITC or AlexaFluor 555, respectively; nuclei were counterstained with Hoechst 33342.[37] Images were analyzed with a Keyence BZ-X700 fluorescence microscope.

Author Manuscript Author Manuscript Author Manuscript Author Manuscript

Bone histomorphometry, TRAP and TUNEL staining

Tibiae were fixed in 70% ethanol, dehydrated, and embedded in methyl-methacrylate and sectioned at the University of Alabama, Birmingham, Center for Metabolic Bone Disease. Some sections were stained with Masson's trichrome, or stained for tartrate-resistant acid phosphatase, while unstained sections were used to assess fluorochrome labeling.[37] TUNEL staining of de-plasticized sections was performed as described.[37] Slides were scanned with a Hamamatsu Nanozoomer 2.0 HT Slide Scanning System, and image analysis was performed using the Nanozoomer Digital Pathology NDP.view2 software. Histomorphometric measurements were performed between 0.25 and 2.25 mm distal to the growth plate as described.[39]

Immunohistochemistry

Femurs were fixed overnight in 10% neutral formalin solution, decalcified in 10% EDTA (pH 7.5) for 5 d, and embedded in paraffin. Sections (8 μm thick) were de-paraffinized in xylene and rehydrated in graded ethanol and water. For antigen retrieval, slides were placed in 10 mM sodium citrate buffer (pH 6.0) at 80–85°C, and allowed to cool to room temperature for 30 min. Endogenous peroxidase activity was quenched in 3% hydrogen peroxide for 10 min. Slides were blocked with 5% normal goat serum and incubated overnight at 4°C with anti-phospho-ERK antibody (1:100 in blocking buffer), followed by HRP-conjugated secondary antibody for 1 h at room temperature. After development with 3,3-diaminobenzidine substrate (Vector Laboratories, Inc., Burlingame, CA), slides were counterstained with hematoxylin.

Micro-CT

Micro-CT analyses were performed on ethanol-fixed tibiae, using a Skyscan 1076 (Kontich, Belgium) scanner at 9 μm voxel size, and applying an electrical potential of 50 kVp and current of 200 μA, with a 0.5 mm aluminum filter, as described.[39] Mineral density was determined by calibration of images against 2 mm diameter hydroxyapatite rods (0.25 and 0.75 g/cm^3). Cortical bone was analyzed by automatic contouring 3.6 mm–4.5 mm distal to the proximal growth plate, using a global threshold to identify cortical bone, and eroding one pixel to eliminate partial volume effects. Trabecular bone was analyzed by automatic contouring of the proximal tibial metaphysis 0.36 –2.1 mm distal to the growth plate and using an adaptive threshold to select the trabecular bone.

Statistical Analyses

Graph Pad Prism 5 was used for two-tailed Student t-test (to compare two groups) or one-way ANOVA with Bonferroni post-test analysis (to compare more than two groups); $p<0.05$ was considered significant. For *in vivo* experiments, we tested our primary hypothesis, that NO-Cbi improves bone architecture and bone formation parameters in OVX (or intact) mice, and our secondary hypothesis that ovariectomy induces bone loss compared to sham-operated animals, using the Student t-test to assess for differences between means of two groups. Based on data variability from previously published studies,[38] we estimated a sample size of six mice would provide 90% power to detect a difference in bone volume fraction (BV/TV) between OVX and sham-operated mice, whereas eight mice per group

Author Manuscript Author Manuscript Author Manuscript Author Manuscript

were required to detect an absolute increase of 0.35% in BV/TV in drug-treated OVX mice with 90% power (α error set at 5%).

RESULTS

NO-Cbi enhances cGMP/PKG and Erk/Akt signaling, gene expression, proliferation, and survival in POBs

We have shown that cobinamide binds NO with high affinity (K_a ~10^{10} M^{-1}), yielding NO-Cbi.[34] NO-Cbi is stable in aqueous solutions for at least 16 h at room temperature, but it releases NO rapidly in the presence of NO scavengers or when added to cells in culture medium.[33] Murine POBs produced nitrite and nitrate—stable NO oxidation products—yielding a medium concentration of ~10 μM after 2 h. Adding NO-Cbi at a final concentration of 10 μM to the cells increased the amount of nitrite and nitrate within 10 min, and, by 30 min, the difference in the concentration of nitrite and nitrate measured in the presence and absence of NO-Cbi reached ~9 μM, indicating that ~90% of the NO bound to NO-Cbi was released (Fig. 1A). NO-Cbi increased the intracellular cGMP concentration in a dose-dependent fashion, resulting in maximal phosphorylation of the PKG substrate vasodilator-stimulated phosphoprotein (VASP) at 3–10 μM (Fig. 1B,C).

We showed previously that estrogens activate Erk and Akt in a NO/cGMP/PKG-dependent manner in osteocytes and osteoblasts, and that activation of these signaling proteins is essential for estrogen's anti-apoptotic effects in osteocytes/blasts.[15] We also showed that the pro-proliferative effects of fluid shear stress on osteoblasts are mediated by NO/cGMP/PKG via Src activation of Erk.[16] Consistent with increasing intracellular cGMP, NO-Cbi increased Erk and Akt phosphorylation in murine POBs, protecting cells from serum starvation-induced apoptosis and stimulating proliferation (Fig. 1D–G). In the POBs, NO-Cbi raised mRNA expression of osteoblast differentiation-related genes, including osteocalcin (OCN), osteopontin (Spp1), collagen1-α1 (Col1a1), alkaline phosphatase (ALP), and low-density lipoprotein receptor-related protein-5 (Lrp5), with tubulin (Tuba1) expression serving as a control for RNA quality (Fig. 1H). NO-Cbi decreased osteoblast expression of RANKL mRNA, whereas it increased expression of the RANKL antagonist OPG, suggesting NO-Cbi could inhibit osteoclast differentiation (Fig. 1I).

NO-Cbi stimulates Wnt signaling and mPOB proliferation via PKG II

The Wnt/β-catenin pathway controls osteoblast differentiation, proliferation, and survival, and is essential for bone mass acquisition and maintenance; increased or decreased gene expression and gain- or loss-of-function mutations of Wnt pathway components cause high *versus* low bone mass phenotypes—for example, expression and activity of the Wnt co-receptor Lrp5 positively correlate with bone mass in humans and mice.[40] Stability and nuclear translocation of β-catenin are negatively controlled by glycogen synthase kinase-3 (GSK-3), which in turn is negatively controlled by phosphorylation on a site targeted by Akt and PKG II.[41, 42] To examine the role of NO and PKG II in osteoblast Wnt signaling, we used POBs isolated from mice which carry floxed PKG II alleles ($PRKG2^{f/f}$ mice), and infected cells with adenovirus encoding CRE recombinase to induce PKG II deficiency (Fig. 2A). In cells infected with control virus encoding LacZ, NO-Cbi induced Akt and GSK-3

Author Manuscript Author Manuscript Author Manuscript Author Manuscript

phosphorylation and β-catenin nuclear translocation, but these effects were largely lost in CRE virus-infected, PKG II-deficient cells (Fig. 2B,C). Similarly, NO-Cbi-induced proliferation was prevented by CRE-mediated PKG II knockout (Fig. 2D). NO-Cbi treatment increased Wnt1a, Lrp5, and β-catenin mRNA expression in the presence, but not in the absence of PKG II (Fig. 2E). Lrp5 protein increased in parallel to mRNA in response to NO-Cbi (Fig. 2F). Transcript levels of the Wnt/β-catenin target genes cyclin D (CycD), ALP, and OCN were increased by NO-Cbi in PKG II-expressing, but not in PKG II-deficient cells (Fig. 2E). The data shown in Fig. 2 are from POBs isolated from $PRKG2^{f/f}$ mice in a mixed S129/C57Bl6 background. Similar experiments were performed in POBs isolated from $PRKG2^{f/f}$ mice back-crossed for five generations into the C57Bl/6 background, yielding nearly identical results (Supplemental Fig. 1). We conclude that NO-Cbi stimulates Wnt/β-catenin signaling in murine POBs via PKG II.

NO-Cbi inhibits osteoclast differentiation

To examine the effect of NO-Cbi on osteoclast differentiation *in vitro*, we cultured adherent murine bone marrow cells with recombinant M-CSF and RANKL.[38] NO-Cbi reduced the number of TRAP-positive osteoclasts, with maximal effects observed at 10 μM (Fig. 3A,B). Less pronounced inhibition was observed with the NO donor DETA-NONOate at a concentration calculated to release equivalent amounts of NO (Fig. 3C). In contrast, the cGMP analog 8-pCPT-cGMP, at a concentration that maximally activated PKG I and II in intact cells, had a smaller, non-significant effect on the number of TRAP-positive cells (Fig. 3C). Consistent with the effects of NO-Cbi on osteoclast differentiation, mRNA expression of the osteoclast-specific genes TRAP, cathepsin K (Ctsk), and calcitonin receptor (CalcR) was markedly reduced in NO-Cbi-treated osteoclast cultures (Fig. 3D).

To determine if the effect of NO-Cbi on osteoclast differentiation required PKG II, we isolated bone marrow cells from $PRKG2^{f/f}$ mice; infecting the cells with CRE adenovirus reduced PRKG2 mRNA expression by > 75% (Fig. 3E). Cells infected with control (GFP) virus or CRE virus produced similar amounts of large, mature, multi-nucleated osteoclasts when cultured in the presence of M-CSF and RANKL, indicating that PKG II is dispensible for osteoclast differentiation (Fig. 3F,G). NO-Cbi inhibited osteoclast differentiation to a similar degree in cells infected with control virus or CRE virus, suggesting a PKG II-independent effect (Fig. 3F.G).

NO-Cbi increases serum cGMP concentration, bone formation, and osteoblastic gene expression in female mice

To test if NO-Cbi could prevent bone manifestations of estrogen deficiency, we subjected sexually-mature, 11 week-old C57Bl/6 mice to bilateral ovariectomy (OVX) or sham operation; we then injected the OVX mice with vehicle or NO-Cbi for five weeks, starting one week postoperatively. We used a NO-Cbi dose (10 mg/kg/d) that had no significant effect on systolic blood pressure and resulted in serum cobinamide concentrations below our limits of detection (<1 μM). Similar to our previous results,[39] OVX mice had lower serum cGMP concentrations compared to sham-operated mice, but NO-Cbi significantly increased the serum cGMP concentration 1 h post administration (Fig. 4A). NO-Cbi reversed the decrease in osteoblast numbers found in OVX mice, and significantly increased mineral

Author Manuscript Author Manuscript Author Manuscript Author Manuscript

apposition rate (MAR), mineralizing surfaces (MS/BS), and bone formation rate (BFR) on trabecular bone surfaces (Fig. 4B–E and Suppl. Fig. 2A). Similarly, NO-Cbi increased MAR and BFR on endocortical surfaces, although endocortical MS/BS was not affected (Suppl. Fig. 2B). Consistent with these results, mRNA expression of osteoblast differentiation-related genes (OCN, Spp1, ALP, Col1a1, and Lrp5) was higher in femoral shafts of NO-Cbi-treated OVX mice compared to vehicle-treated OVX mice, whereas tubulin-α1 mRNA was unchanged (Fig. 4F).

In a separate experiment, we examined the effects of NO-Cbi in 12 week-old, intact female mice. Treating the mice with NO-Cbi at 10 mg/kg/d for five weeks increased the serum cGMP concentration, osteoblast numbers, and MAR and BFR in trabecular bone, similar to results found in OVX mice (Fig. 4G–K and Suppl. Fig. 2C). We saw no effect of NO-Cbi on cortical bone formation parameters in intact mice (Suppl. Fig. 2D). NO-Cbi increased mRNA expression of OCN and ALP in intact mice, and showed a trend toward increased Col1a1 mRNA expression, but, in contrast to OVX mice, NO-Cbi did not affect Spp1 and Lrp5 mRNA in intact mice (Fig. 4L). These results indicate that NO-Cbi increases osteoblastic activity not only in OVX mice, but also in the presence of physiological estrogen concentrations.

NO-Cbi prevents estrogen deficiency-induced osteocyte apoptosis

Estrogen deficiency-induced bone loss is associated with osteocyte apoptosis.[11, 12, 39, 43] Osteocyte death induces local bone remodeling via osteoclast recruitment,[12] and targeted osteocyte ablation *in vivo* causes osteoporosis, as shown in an osteocyte-specific diphtheria toxin receptor mouse model.[44] Prevention of OVX-induced bone loss by estrane, which lacks estrogen's transcriptional effects and reduces osteoclast numbers less effectively than estrogen, may be partly due to estrane protecting osteocytes from apoptosis.[45]

We showed previously that the pro-survival effects of estrogen in osteocytes require NO/cGMP/PKG signaling, and are at least partly dependent on Erk activation.[15] Consistent with previous reports,[15, 39, 43] we saw a significant increase in TUNEL-positive, apoptotic osteocytes in trabecular and cortical bone of OVX mice, with NO-Cbi reducing osteocyte apoptosis to values found in sham-operated mice (Fig. 5A–C, Suppl. Fig. 3 for cortical bone). Similar results were obtained when we examined the amount of cleaved caspase-3 in bone lysates from NO-Cbi- *versus* vehicle-treated OVX mice (Fig. 5D). Immunohistochemical staining of pErk was evident in bone-lining osteoblastic cells of sham-operated mice, but was faint or absent in OVX mice; treating OVX mice with NO-Cbi induced prominent pErk staining in bone-lining cells (Fig. 5E; isotype-matched control immunoglobulin produced no staining, data not shown).

NO-Cbi regulates RANKL/OPG expression and reduces osteoclasts in female mice

Estrogens reduce osteoclast survival,[9, 46] and, similar to findings by other workers, we found an increased number of TRAP-positive osteoclasts on trabecular bone in the OVX mice (Fig. 6A,B; few osteoclasts were seen on cortical surfaces under all conditions). Treating OVX mice with NO-Cbi reduced osteoclast numbers to values found in sham-operated animals (Fig. 6A,B). Compared to vehicle-treated OVX mice, femurs of NO-Cbi-treated OVX mice

Author Manuscript Author Manuscript Author Manuscript Author Manuscript

contained less RANKL and more OPG mRNA, and mRNA expression of the osteoclast marker genes CTSK and TRAP was decreased (Fig. 6C). Similarly, NO-Cbi decreased RANKL mRNA, osteoclast numbers, and osteoclastic marker genes in intact mice (Fig. 6D,E). Thus, NO-Cbi reduced osteoclast numbers and osteoclastic gene expression in both intact and OVX mice, in part, by reducing the RANKL/OPG ratio, and, in part, by directly inhibiting osteoclast differentiation (Fig. 3).

NO-Cbi increases trabecular bone mass in female mice

We examined the effects of NO-Cbi on tibial bone microarchitecture by micro-CT. Consistent with previous reports,[39, 47] OVX mice had significantly lower trabecular bone volume, trabecular number, and trabecular BMD compared to sham-operated mice; NO-Cbi partly restored all three parameters (Fig. 7A–D). Similarly, NO-Cbi treatment increased trabecular bone volume and BMD in intact mice, although the effect on trabecular number did not reach significance (Fig. 7E–G). We found no difference in cortical thickness or cortical tissue mineral density between sham-operated and OVX mice, and NO-Cbi did not affect cortical bone parameters in OVX or intact mice (Suppl. Fig. 4). Since we performed ovariectomies in young mice before they achieved peak bone mass, the reduced trabecular bone mass in the OVX mice represents a failure to gain bone, rather than bone loss.[48] Estrogen deficiency-induced changes in trabecular bone mass are typically more pronounced than changes in cortical bone mass, with cortical changes taking longer than trabecular changes and varying with age and mouse strain.[39, 47, 49–51]

DISCUSSION

A better understanding of the molecular mechanisms controlling bone homeostasis has led to development of multiple drugs for osteoporosis that inhibit bone resorption by targeting osteoclast differentiation and/or function.[2, 5] However, the only clinically-available agents that stimulate osteoblast activity and bone formation are PTH analogs, but they also stimulate osteoclasts, limiting their effectiveness.[2, 5] Therefore, agents that simultaneously stimulate osteoblast and inhibit osteoclast functions are needed. We found that the NO donor NO-Cbi improved trabecular bone architecture and increased bone formation markers in intact female mice and OVX mice, while dramatically decreasing osteoclasts. Our results confirm bone-anabolic effects of NO, explore mechanisms of NO actions in bone cells, and demonstrate *in vitro* and *in vivo* effectiveness of a novel, direct NO-releasing agent.

An important role of NO in osteoblast biology is supported by rodent studies: NOS3-deficient mice have reduced bone mass due to defects in osteoblast number and maturation, and show exaggerated bone loss after ovariectomy, with a blunted response to estrogens[52–54]. Moreover, NO-generating organic nitrates improve BMD in estrogen-deficient rats (as measured by DXA), whereas NOS inhibitors block estrogen's bone-protective effects and prevent bone formation induced by mechanical stimulation in rodents.[17, 18, 23, 24, 55] In humans and rats, serum concentrations of the NO metabolites nitrite and nitrate correlate with estradiol concentrations, and increase with estrogen administration.[24, 56] Estrogen deficiency reduces NOS expression and activity, leading to a state of relative NO- and, consequently, cGMP-deficiency.[39, 57] NO-Cbi restored serum

Author Manuscript Author Manuscript Author Manuscript Author Manuscript

cGMP concentrations in OVX mice, and the drug's positive effects on osteoblast proliferation, differentiation, and survival were likely mediated via increased intracellular cGMP concentrations and PKG activation, because the drug increased Wnt/β-catenin signaling in a PKG II-dependent fashion. We have shown previously that cGMP-elevating agents and cGMP analogs increase osteoblast proliferation, differentiation, and survival, with PKG II activation of Src required for Erk and Akt activation, and PKG I phosphorylation of Bcl-2 contributing to anti-apoptotic effects in osteoblasts and osteocytes.[15, 16, 39] Consistent with its *in vitro* effects on POBs, NO-Cbi increased osteoblast number, osteoblastic gene expression, mineral apposition and bone formation rates, and trabecular bone volume and BMD in intact female and OVX mice, while reducing osteocyte apoptosis in OVX mice. Like NO-Cbi, the NO-independent soluble guanylate cyclase activator cinaciguat increased bone formation and osteoblast marker genes and improved trabecular bone architecture in OVX mice; however, in contrast to NO-Cbi, cinciguat did not modify trabecular bone volume or BMD in intact mice and had minimal non-significant effects on osteoclasts.[39]

NO appears to have dual functions in osteoclast biology: low NO concentrations generated by NOS1 promote, while higher NO concentrations generated by NOS2 inhibit osteoclast differentiation and survival.[58, 59] NOS1-deficient mice have increased bone mass with reduced bone turnover due to defects in osteoclast differentiation and function, indicating a positive role of NO in osteoclasts.[58, 60] However, RANKL induction of NOS2 inhibits RANKL-induced osteoclast differentiation, and NOS2-deficient osteoclasts show increased differentiation in response to RANKL.[59] Adding NO donors to mature osteoclasts inhibits their resorptive activity.[61–63]

NO-Cbi decreased osteoclast numbers and reduced osteoclast-specific TRAP and CTSK mRNAs in bones of intact and OVX mice, correlating with a decreased RANKL/OPG mRNA ratio in bone. In contrast, the cGMP-elevating agent cinaciguat did not influence osteoclast numbers, osteoclast-specific genes, RANKL, or OPG in OVX or sham-operated mice.[39] In agreement with these *in vivo* results, NO-Cbi reduced RANKL and increased OPG mRNA in cultured POBs, whereas cinaciguat did not affect these genes.[39] RANKL and OPG are key regulators of osteoclast differentiation, produced primarily by osteoblastic-type cells.[2] Other workers have shown down-regulation of RANKL by NO, but not by cGMP analogs, in bone marrow stromal cells.[64] In addition to reducing the RANKL/OPG ratio in bone and POBs, NO-Cbi directly inhibited osteoclast differentiation *in vitro,* in the presence of excess RANKL and M-CSF. A cGMP analog had little effect on osteoclast differentiation, and the NO-Cbi effect was independent of PKG II. cGMP-independent NO effects on osteoclast differentiation have been reported previously;[59, 65] however, cGMP may inhibit mature osteoclast functions, such as acid secretion and motility, in a PKG I-dependent manner.[66, 67]

Epidemiological data link the use of organic nitrates (i.e., nitroglycerin and isosorbide mononitrate) to reduced fracture risk,[20–22] and two prospective, randomized trials showed a positive effect of nitrates on BMD, at doses lower than those used for vasodilation: in young women who underwent ovariectomy, nitroglycerin was as effective as estrogen replacement in preventing bone loss,[25] and, in post-menopausal women with established osteoporosis,

Author Manuscript Author Manuscript Author Manuscript Author Manuscript

iso-sorbide mononitrate improved BMD as effectively as a bisphosphonate.[26] In addition, in healthy post-menopausal women, isosorbide mononitrate decreased a bone resorption marker (N-terminal telopeptide) and increased a bone formation marker (alkaline phosphatase).[68] However, a large trial in post-menopausal women failed to show an effect of nitroglycerin on BMD, possibly because treatment adherence was poor.[27]

Organic nitrates must be activated by mitochondrial aldehyde dehydrogenase, which leads to oxidative stress, development of tolerance, and endothelial dysfunction,[29, 30] and several large trials of chronic nitrate use in patients with coronary artery disease showed increased mortality in treated patients,[69, 70,28] Since oxidative stress is implicated in the pathophysiology of estrogen deficiency- and age-related osteoporosis,[10] and can lead to decreased NO bio-availability and soluble guanylate cyclase desensitization,[31] the beneficial effects of nitrates in post-menopausal osteoporosis are likely limited by their pro-oxidant properties.

Considerable effort has been directed towards developing second generation, direct NO-releasing agents, but to date, none have shown efficacy in clinical trials, and some generate toxic metabolites in the process of NO release, making them unsuitable for clinical use.[31, 71] We have developed NO-Cbi as a novel, direct NO donor with major advantages over existing, FDA-approved nitrates. NO-Cbi is derived from the penultimate vitamin B_{12} precursor cobinamide, which is present at low concentrations in human serum. We have found in rodents that cobinamide has no toxicity at >50-fold higher doses than those used in this study and those required for delivery of pharmacological amounts of NO (G.R. Boss et al., unpublished data and[33]). After NO release, cobinamide is generated, and cobinamide can bind O_2^- and other reactive oxygen species,[36] providing a potential added benefit of protecting cells from oxidative stress. Repeated administration of NO-Cbi does not induce tolerance, and NO-Cbi is stable and can be administered by multiple routes, including oral ingestion (G.R. Boss et al., unpublished data, and[33]).

A limitation of our study is that ovariectomy in young mice does not mimic the gradual cessation of ovarian function occurring during menopause. However, OVX mice are an accepted model of estrogen deficiency-induced osteoporosis, and show changes in bone architecture and turnover similar to those observed in post-menopausal women, including increased bone resorption and increased osteoblast/osteocyte apoptosis.[9, 43, 47, 51] Some workers have observed increased bone formation markers in parallel with increased resorption in OVX mice, whereas we and others found no change in mineral apposition rate and a trend towards reduced mineralizing surface and bone formation rate after OVX.[72–75] These differences may be attributable to differences in mouse strain and age, the type of bone examined, and the time interval after OVX. We did not observe changes in cortical bone post OVX, but OVX-induced cortical changes vary greatly among different inbred mouse strains, with age of the mice, the site examined, and the time interval after surgery.[39, 47, 49–51] Another limitation of our study is that we examined a single NO-Cbi dose; this dose was chosen based on its lack of effect on systolic blood pressure. Further studies are needed to optimize treatment dose and schedule, and to test the effect of oral NO-Cbi.

Author Manuscript Author Manuscript Author Manuscript Author Manuscript

In conclusion, we found that NO-Cbi regulates bone remodeling by promoting osteoblast proliferation, differentiation, and survival, while inhibiting osteoclast differentiation directly and indirectly (via RANKL). NO-Cbi improved bone mass in OVX mice, a frequently-used model of post-menopausal osteoporosis, as well as in intact female mice.[9, 47, 76] We are unaware of previous work using a direct NO-releasing agent as a bone-anabolic agent in animals or humans.

Supplementary Material

Refer to Web version on PubMed Central for supplementary material.

Acknowledgments

We are grateful to Ella Kothari, Jennifer Santini, Dana Smith, and Dezhi Wang for their expert assistance. This work was supported by NIH grants R01-AR051300 and R21-AR065658 (to RBP); U01-NS58030 (to GRB, CounterACT Program, Office of the Director, NIH and NINDS), P01-AG007996 (RLS), P30-CA023100 (UCSD Gene Targeting and Transgenic Mouse Core), P30-NS047101 (UCSD Neuroscience Microscopy Shared Facility), and P30-AR04603 (University of Alabama, Birmingham, Center for Metabolic Bone Disease). NS was supported by the Deutsche Forschungsgemeinschaft (Project KI 1303/2-1).

Authors' roles: Study design: RBP and GRB. Study conduct: HK, GR, JJ, NS, EC, and DC. Data collection: HK, GR and EC. Data analysis: HK, GR, and RBP. Data interpretation: RBP, HK, GRB, and RS. Drafting manuscript: HK and RBP. RBP and HK take responsibility for the integrity of the data analysis.

References

1. Dallas SL, Prideaux M, Bonewald LF. The osteocyte: an endocrine cell… and more. Endocr Rev. 2013; 34(5):658–90. [PubMed: 23612223]
2. Kawai M, Modder UI, Khosla S, Rosen CJ. Emerging therapeutic opportunities for skeletal restoration. Nat Rev Drug Discov. 2011; 10(2):141–56. [PubMed: 21283108]
3. Watts NB, Bilezikian JP, Camacho PM, Greenspan SL, Harris ST, Hodgson SF, Kleerekoper M, Luckey MM, McClung MR, Pollack RP, Petak SM. American Association of Clinical Endocrinologists Medical Guidelines for Clinical Practice for the diagnosis and treatment of postmenopausal osteoporosis. Endocr Pract. 2010; 16(Suppl 3):1–37.
4. Khosla S, Bellido TM, Drezner MK, Gordon CM, Harris TB, Kiel DP, Kream BE, LeBoff MS, Lian JB, Peterson CA, Rosen CJ, Williams JP, Winer KK, Sherman SS. Forum on aging and skeletal health: summary of the proceedings of an ASBMR workshop. J Bone Miner Res. 2011; 26(11): 2565–78. [PubMed: 21915901]
5. Reid IR. Short-term and long-term effects of osteoporosis therapies. Nat Rev Endocrinol. 2015; 11(7):418–28. [PubMed: 25963272]
6. Neer RM, Arnaud CD, Zanchetta JR, Prince R, Gaich GA, Reginster JY, Hodsman AB, Eriksen EF, Ish-Shalom S, Genant HK, Wang O, Mitlak BH. Effect of parathyroid hormone (1-34) on fractures and bone mineral density in postmenopausal women with osteoporosis. N Engl J Med. 2001; 344(19):1434–41. [PubMed: 11346808]
7. Barrett-Connor E, Grady D, Stefanick ML. The rise and fall of menopausal hormone therapy. Annu Rev Public Health. 2005; 26:115–40. [PubMed: 15760283]
8. Barrett-Connor E, Wade SW, Do TP, Satram-Hoang S, Stewart R, Gao G, Macarios D. Treatment satisfaction and persistence among postmenopausal women on osteoporosis medications: 12-month results from POSSIBLE US. Osteoporos Int. 2012; 23(2):733–41. [PubMed: 21625886]
9. Khosla S, Melton LJ III, Riggs BL. The unitary model for estrogen deficiency and the pathogenesis of osteoporosis: is a revision needed? J Bone Miner Res. 2011; 26(3):441–51. [PubMed: 20928874]
10. Manolagas SC. From estrogen-centric to aging and oxidative stress: a revised perspective of the pathogenesis of osteoporosis. Endocr Rev. 2010; 31(3):266–300. [PubMed: 20051526]

Author Manuscript Author Manuscript Author Manuscript Author Manuscript

11. Tomkinson A, Reeve J, Shaw RW, Noble BS. The death of osteocytes via apoptosis accompanies estrogen withdrawal in human bone. J Clin Endocrinol Metab. 1997; 82(9):3128–35. [PubMed: 9284757]
12. Emerton KB, Hu B, Woo AA, Sinofsky A, Hernandez C, Majeska RJ, Jepsen KJ, Schaffler MB. Osteocyte apoptosis and control of bone resorption following ovariectomy in mice. Bone. 2010; 46(3):577–83. [PubMed: 19925896]
13. Ozcivici E, Luu YK, Adler B, Qin YX, Rubin J, Judex S, Rubin CT. Mechanical signals as anabolic agents in bone. Nat Rev Rheumatol. 2010; 6(1):50–9. [PubMed: 20046206]
14. Rangaswami H, Marathe N, Zhuang S, Chen Y, Yeh JC, Frangos JA, Boss GR, Pilz RB. Type II cGMP-dependent protein kinase mediates osteoblast mechanotransduction. J Biol Chem. 2009; 284:14796–808. [PubMed: 19282289]
15. Marathe N, Rangaswami H, Zhuang S, Boss GR, Pilz RB. Pro-survival Effects of 17beta-Estradiol on Osteocytes Are Mediated by Nitric Oxide/cGMP via Differential Actions of cGMP-dependent Protein Kinases I and II. J Biol Chem. 2012; 287(2):978–88. [PubMed: 22117068]
16. Rangaswami H, Schwappacher R, Marathe N, Zhuang S, Casteel DE, Haas B, Chen Y, Pfeifer A, Kato H, Shattil S, Boss GR, Pilz RB. Cyclic GMP and protein kinase G control a Src-containing mechanosome in osteoblasts. Sci Signal. 2010; 3(153):ra91. [PubMed: 21177494]
17. Samuels A, Perry MJ, Gibson RL, Colley S, Tobias JH. Role of endothelial nitric oxide synthase in estrogen-induced osteogenesis. Bone. 2001; 29(1):24–9. [PubMed: 11472887]
18. Turner CH, Owan I, Jacob DS, McClintock R, Peacock M. Effects of nitric oxide synthase inhibitors on bone formation in rats. Bone. 1997; 21(6):487–90. [PubMed: 9430237]
19. Fox SW, Chambers TJ, Chow JW. Nitric oxide is an early mediator of the increase in bone formation by mechanical stimulation. Am J Physiol. 1996; 270(6 Pt 1):E955–E960. [PubMed: 8764178]
20. Rejnmark L, Vestergaard P, Mosekilde L. Decreased fracture risk in users of organic nitrates: a nationwide case-control study. J Bone Miner Res. 2006; 21(11):1811–7. [PubMed: 17054422]
21. Pouwels S, Lalmohamed A, van ST, Cooper C, Souverein P, Leufkens HG, Rejnmark L, de BA, Vestergaard P, de VF. Use of organic nitrates and the risk of hip fracture: a population-based case-control study. J Clin Endocrinol Metab. 2010; 95(4):1924–31. [PubMed: 20130070]
22. Jamal SA, Browner WS, Bauer DC, Cummings SR. Intermittent use of nitrates increases bone mineral density: the study of osteoporotic fractures. J Bone Miner Res. 1998; 13(11):1755–9. [PubMed: 9797485]
23. Wimalawansa SJ, De MG, Gangula P, Yallampalli C. Nitric oxide donor alleviates ovariectomy-induced bone loss. Bone. 1996; 18(4):301–4. [PubMed: 8726385]
24. Hukkanen M, Platts LA, Lawes T, Girgis SI, Konttinen YT, Goodship AE, MacIntyre I, Polak JM. Effect of nitric oxide donor nitroglycerin on bone mineral density in a rat model of estrogen deficiency-induced osteopenia. Bone. 2003; 32(2):142–9. [PubMed: 12633786]
25. Wimalawansa SJ. Nitroglycerin therapy is as efficacious as standard estrogen replacement therapy (Premarin) in prevention of oophorectomy-induced bone loss: a human pilot clinical study. J Bone Miner Res. 2000; 15(11):2240–4. [PubMed: 11092405]
26. Nabhan AF, Rabie NH. Isosorbide mononitrate versus alendronate for postmenopausal osteoporosis. Int J Gynaecol Obstet. 2008; 103(3):213–6. [PubMed: 18805524]
27. Wimalawansa SJ, Grimes JP, Wilson AC, Hoover DR. Transdermal nitroglycerin therapy may not prevent early postmenopausal bone loss. J Clin Endocrinol Metab. 2009; 94(9):3356–64. [PubMed: 19549739]
28. Thomas GR, DiFabio JM, Gori T, Parker JD. Once daily therapy with isosorbide-5-mononitrate causes endothelial dysfunction in humans: evidence of a free-radical-mediated mechanism. J Am Coll Cardiol. 2007; 49(12):1289–95. [PubMed: 17394960]
29. Munzel T, Wenzel P, Daiber A. Do we still need organic nitrates? J Am Coll Cardiol. 2007; 49(12): 1296–8. [PubMed: 17394961]
30. Parker JD. Nitrate tolerance, oxidative stress, and mitochondrial function: another worrisome chapter on the effects of organic nitrates. J Clin Invest. 2004; 113(3):352–4. [PubMed: 14755331]
31. Lundberg JO, Gladwin MT, Weitzberg E. Strategies to increase nitric oxide signalling in cardiovascular disease. Nat Rev Drug Discov. 2015; 14(9):623–41. [PubMed: 26265312]

Author Manuscript Author Manuscript Author Manuscript Author Manuscript

32. Sydow K, Daiber A, Oelze M, Chen Z, August M, Wendt M, Ullrich V, Mulsch A, Schulz E, Keaney JF Jr, Stamler JS, Munzel T. Central role of mitochondrial aldehyde dehydrogenase and reactive oxygen species in nitroglycerin tolerance and cross-tolerance. J Clin Invest. 2004; 113(3): 482–9. [PubMed: 14755345]
33. Broderick KE, Alvarez L, Balasubramanian M, Belke DD, Makino A, Chan A, Woods VL Jr, Dillmann WH, Sharma VS, Pilz RB, Bigby TD, Boss GR. Nitrosyl-cobinamide, a new and direct nitric oxide-releasing drug effective *in vivo*. Exp Biol Med (Maywood). 2007; 232(11):1432–40. [PubMed: 18040067]
34. Sharma VS, Pilz RB, Boss GB, Magde D. Reactions of nitric oxide with vitamin B12 and its precursor, cobinamide. Biochemistry. 2003; 42:8900–8. [PubMed: 12873151]
35. Spitler R, Schwappacher R, Wu T, Kong X, Yokomori K, Pilz RB, Boss GR, Berns MW. Nitrosyl-cobinamide (NO-Cbi), a new nitric oxide donor, improves wound healing through cGMP/cGMP-dependent protein kinase. Cell Signal. 2013; 25(12):2374–82. [PubMed: 23920342]
36. Jiang J, Chan A, Ali S, Saha A, Haushalter K, Lam M, Glasheen M, Parker J, Brenner M, Mahon-Brenner S, Patel H, Ambasudhan R, Lipton S, Pilz R, Boss G. Hydrogen sulfide-mechanisms of toxicity and development of an antidote. Scientific Reports. 2016; 6:20831. [PubMed: 26877209]
37. Kalyanaraman H, Schwappacher R, Joshua J, Zhuang S, Scott BT, Klos M, Casteel DE, Frangos JA, Dillmann W, Boss GR, Pilz RB. Nongenomic thyroid hormone signaling occurs through a plasma membrane-localized receptor. Sci Signal. 2014; 7(326):ra48. [PubMed: 24847117]
38. Takahashi, N.; Udagawa, N.; Tanaka, S.; Suda, T. Generating murine osteoblasts from bone marrow. In: Helfrich, MH.; Ralston, SH., editors. Methods in Molecula Medicine, Vol. 80: Bone Research Protocols. Totowa, NJ: Humana Press Inc; 2003. p. 129-44.
39. Joshua J, Schwaerzer GK, Kalyanaraman H, Cory E, Sah RS, Li M, Vaida F, Boss GR, Pilz RB. Soluble guanylate cyclase as a novel treatment target for osteoporosis. Endocrinology. 2014; 155(12):4720–30. [PubMed: 25188528]
40. Baron R, Kneissel M. WNT signaling in bone homeostasis and disease: from human mutations to treatments. Nat Med. 2013; 19(2):179–92. [PubMed: 23389618]
41. Cohen P, Frame S. The renaissance of GSK3. Nature Rev Mol Cell Biol. 2001; 2(10):769–76. [PubMed: 11584304]
42. Zhao X, Zhuang S, Chen Y, Boss GR, Pilz RB. Cyclic GMP-dependent protein kinase regulates CCAAT enhancer-binding protein beta functions through inhibition of glycogen synthase kinase-3. J Biol Chem. 2005; 280:32683–92. [PubMed: 16055922]
43. Kousteni S, Bellido T, Plotkin LI, O'Brien CA, Bodenner DL, Han L, Han K, DiGregorio GB, Katzenellenbogen JA, Katzenellenbogen BS, Roberson PK, Weinstein RS, Jilka RL, Manolagas SC. Nongenotropic, sex-nonspecific signaling through the estrogen or androgen receptors: dissociation from transcriptional activity. Cell. 2001; 104(5):719–30. [PubMed: 11257226]
44. Tatsumi S, Ishii K, Amizuka N, Li M, Kobayashi T, Kohno K, Ito M, Takeshita S, Ikeda K. Targeted ablation of osteocytes induces osteoporosis with defective mechanotransduction. Cell Metab. 2007; 5(6):464–75. [PubMed: 17550781]
45. Kousteni S, Chen JR, Bellido T, Han L, Ali AA, O'Brien CA, Plotkin L, Fu Q, Mancino AT, Wen Y, Vertino AM, Powers CC, Stewart SA, Ebert R, Parfitt AM, Weinstein RS, Jilka RL, Manolagas SC. Reversal of bone loss in mice by nongenotropic signaling of sex steroids. Science. 2002; 298(5594):843–6. [PubMed: 12399595]
46. Nakamura T, Imai Y, Matsumoto T, Sato S, Takeuchi K, Igarashi K, Harada Y, Azuma Y, Krust A, Yamamoto Y, Nishina H, Takeda S, Takayanagi H, Metzger D, Kanno J, Takaoka K, Martin TJ, Chambon P, Kato S. Estrogen prevents bone loss via estrogen receptor alpha and induction of Fas ligand in osteoclasts. Cell. 2007; 130(5):811–23. [PubMed: 17803905]
47. Bouxsein ML, Myers KS, Shultz KL, Donahue LR, Rosen CJ, Beamer WG. Ovariectomy-induced bone loss varies among inbred strains of mice. J Bone Miner Res. 2005; 20(7):1085–92. [PubMed: 15940361]
48. Brodt MD, Ellis CB, Silva MJ. Growing C57Bl/6 mice increase whole bone mechanical properties by increasing geometric and material properties. J Bone Miner Res. 1999; 14(12):2159–66. [PubMed: 10620076]

Author Manuscript Author Manuscript Author Manuscript Author Manuscript

49. Bartell SM, Han L, Kim HN, Kim SH, Katzenellenbogen JA, Katzenellenbogen BS, Chambliss KL, Shaul PW, Roberson PK, Weinstein RS, Jilka RL, Almeida M, Manolagas SC. Non-nuclear-initiated actions of the estrogen receptor protect cortical bone mass. Mol Endocrinol. 2013; 27(4): 649–56. [PubMed: 23443267]
50. Li CY, Schaffler MB, Wolde-Semait HT, Hernandez CJ, Jepsen KJ. Genetic background influences cortical bone response to ovariectomy. J Bone Miner Res. 2005; 20(12):2150–8. [PubMed: 16294268]
51. Syed FA, Modder UI, Roforth M, Hensen I, Fraser DG, Peterson JM, Oursler MJ, Khosla S. Effects of chronic estrogen treatment on modulating age-related bone loss in female mice. J Bone Miner Res. 2010; 25(11):2438–46. [PubMed: 20499336]
52. Aguirre J, Buttery L, O'Shaughnessy M, Afzal F, de Marticorena IF, Hukkanen M, Huang P, Maclntyre I, Polak J. Endothelial nitric oxide synthase gene-deficient mice demonstrate marked retardation in postnatal bone formation, reduced bone volume, and defects in osteoblast maturation and activity. Am J Pathol. 2001; 158:247–57. [PubMed: 11141498]
53. Armour KE, Armour KJ, Gallagher ME, Godecke A, Helfrich MH, Reid DM, Ralston SH. Defective bone formation and anabolic response to exogenous estrogen in mice with targeted disruption of endothelial nitric oxide synthase. Endocrinology. 2001; 142(2):760–6. [PubMed: 11159848]
54. Grassi F, Fan X, Rahnert J, Weitzmann MN, Pacifici R, Nanes MS, Rubin J. Bone re/modeling is more dynamic in the endothelial nitric oxide synthase(−/−) mouse. Endocrinology. 2006; 147(9): 4392–9. [PubMed: 16763060]
55. Chow JW, Fox SW, Lean JM, Chambers TJ. Role of nitric oxide and prostaglandins in mechanically induced bone formation. J Bone Miner Res. 1998; 13(6):1039–44. [PubMed: 9626636]
56. Hamilton CJ, Reid LS, Jamal SA. Organic nitrates for osteoporosis: an update. Bonekey Rep. 2013; 2:259. [PubMed: 24422039]
57. Mendelsohn ME, Karas RH. Rapid progress for non-nuclear estrogen receptor signaling. J Clin Invest. 2010; 120(7):2277–9. [PubMed: 20577045]
58. van't Hof RJ, Macphee J, Libouban H, Helfrich MH, Ralston SH. Regulation of bone mass and bone turnover by neuronal nitric oxide synthase. Endocrinology. 2004; 145(11):5068–74. [PubMed: 15297441]
59. Zheng H, Yu X, Collin-Osdoby P, Osdoby P. RANKL stimulates inducible nitric-oxide synthase expression and nitric oxide production in developing osteoclasts. An autocrine negative feedback mechanism triggered by RANKL-induced interferon-beta via NF-kappaB that restrains osteoclastogenesis and bone resorption. J Biol Chem. 2006; 281(23):15809–20. [PubMed: 16613848]
60. Jung JY, Lin AC, Ramos LM, Faddis BT, Chole RA. Nitric oxide synthase I mediates osteoclast activity in vitro and in vivo. J Cell Biochem. 2003; 89(3):613–21. [PubMed: 12761894]
61. Dong SS, Williams JP, Jordan SE, Cornwell T, Blair HC. Nitric oxide regulation of cGMP production in osteoclasts. J Cell Biochem. 1999; 73(4):478–87. [PubMed: 10733342]
62. Fuller K, Kirstein B, Chambers TJ. Murine osteoclast formation and function: differential regulation by humoral agents. Endocrinology. 2006; 147(4):1979–85. [PubMed: 16384864]
63. Yaroslavskiy BB, Turkova I, Wang Y, Robinson LJ, Blair HC. Functional osteoclast attachment requires inositol-1,4,5-trisphosphate receptor-associated cGMP-dependent kinase substrate. Lab Invest. 2010; 90:1533–42. [PubMed: 20567233]
64. Fan X, Roy E, Zhu L, Murphy TC, ckert-Bicknell C, Hart CM, Rosen C, Nanes MS, Rubin J. Nitric oxide regulates receptor activator of nuclear factor-kappaB ligand and osteoprotegerin expression in bone marrow stromal cells. Endocrinology. 2004; 145(2):751–9. [PubMed: 14563699]
65. Ralston SH, Grabowski PS. Mechanisms of cytokine induced bone resorption: role of nitric oxide, cyclic guanosine monophosphate, and prostaglandins. Bone. 1996; 19(1):29–33. [PubMed: 8830984]

Author Manuscript Author Manuscript Author Manuscript Author Manuscript

66. Yaroslavskiy BB, Li Y, Ferguson DJ, Kalla SE, Oakley JI, Blair HC. Autocrine and paracrine nitric oxide regulate attachment of human osteoclasts. J Cell Biochem. 2004; 91(5):962–72. [PubMed: 15034931]

67. Yaroslavskiy BB, Zhang Y, Kalla SE, Garcia P V, Sharrow AC, Li Y, Zaidi M, Wu C, Blair HC. NO-dependent osteoclast motility: reliance on cGMP-dependent protein kinase I and VASP. J Cell Sci. 2005; 118(Pt 23):5479–87. [PubMed: 16291726]

68. Jamal SA, Cummings SR, Hawker GA. Isosorbide mononitrate increases bone formation and decreases bone resorption in postmenopausal women: a randomized trial. J Bone Miner Res. 2004; 19(9):1512–7. [PubMed: 15312252]

69. Nakamura Y, Moss AJ, Brown MW, Kinoshita M, Kawai C. Long-term nitrate use may be deleterious in ischemic heart disease: A study using the databases from two large-scale postinfarction studies. Multicenter Myocardial Ischemia Research Group. Am Heart J. 1999; 138(3 Pt 1):577–85. [PubMed: 10467211]

70. Ishikawa K, Kanamasa K, Ogawa I, Takenaka T, Naito T, Kamata N, yamamoto T, Nakai S, Hama J, Oyaizu M, Kimura A, Yamamoto K, Aso N, Arai M, Yabushita H, Katori Y. Long-term nitrate treatment increases cardiac events in patients with healed myocardial infarction. Secondary Prevention Group. Jpn Circ J. 1996; 60(10):779–88. [PubMed: 8933241]

71. Miller MR, Megson IL. Recent developments in nitric oxide donor drugs. Br J Pharmacol. 2007; 151(3):305–21. [PubMed: 17401442]

72. Modder UI, Sanyal A, Kearns AE, Sibonga JD, Nishihara E, Xu J, O'Malley BW, Ritman EL, Riggs BL, Spelsberg TC, Khosla S. Effects of loss of steroid receptor coactivator-1 on the skeletal response to estrogen in mice. Endocrinology. 2004; 145(2):913–21. [PubMed: 14563705]

73. Hayashi M, Nakashima T, Taniguchi M, Kodama T, Kumanogoh A, Takayanagi H. Osteoprotection by semaphorin 3A. Nature. 2012; 485(7396):69–74. [PubMed: 22522930]

74. Duque G, Huang DC, Dion N, Macoritto M, Rivas D, Li W, Yang XF, Li J, Lian J, Marino FT, Barralet J, Lascau V, Deschenes C, Ste-Marie LG, Kremer R. Interferon-gamma plays a role in bone formation in vivo and rescues osteoporosis in ovariectomized mice. J Bone Miner Res. 2011; 26(7):1472–83. [PubMed: 21308779]

75. Pierroz DD, Bonnet N, Baldock PA, Ominsky MS, Stolina M, Kostenuik PJ, Ferrari SL. Are osteoclasts needed for the bone anabolic response to parathyroid hormone? A study of intermittent parathyroid hormone with denosumab or alendronate in knock-in mice expressing humanized RANKL. J Biol Chem. 2010; 285(36):28164–73. [PubMed: 20558734]

76. Syed FA, Melim T. Rodent models of aging bone: an update. Curr Osteoporos Rep. 2011; 9(4): 219–28. [PubMed: 21918858]

Author Manuscript Author Manuscript Author Manuscript Author Manuscript

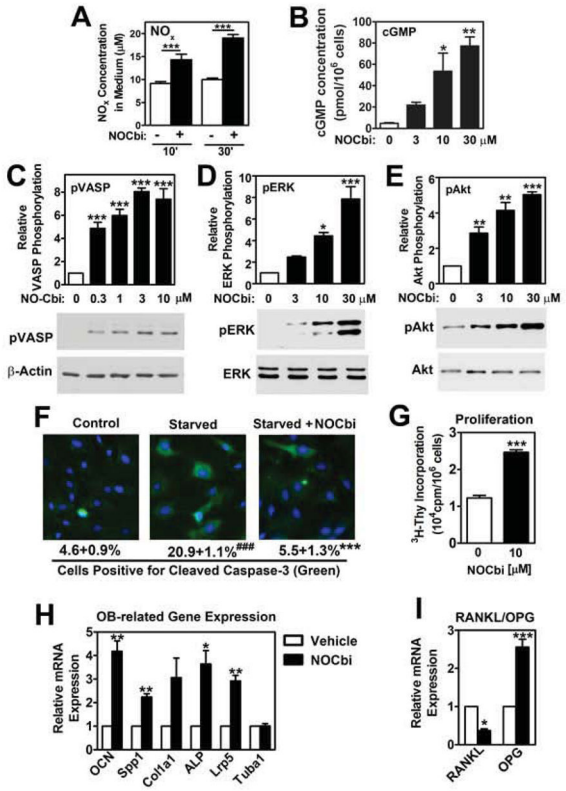

Figure 1. NO-Cbi enhances cGMP/PKG and Erk/Akt signaling, gene expression, proliferation, and survival in POBs

(A) POBs isolated from intact C57Bl6 mice were incubated in medium with 0.1% FBS (3×10^5 cells/ml) for 2 h prior to receiving vehicle or 10 μM NO-Cbi (NOCbi) for the indicated times. Stable NO oxidation products (nitrite plus nitrate, NO_x) were measured in the medium by the Griess reaction (NO_x present in medium without cells was subtracted). **(B,C)** POBs were treated with vehicle or NO-Cbi at the indicated concentrations for 30 min. The intracellular cGMP concentration was measured by ELISA (B), and VASP phosphorylation was analyzed by Western blot using a phospho-Ser^{259}-specific antibody, with bar graph showing densitometric quantification of pVASP normalized to β-actin (C). **(D,E)** Serum-deprived POBs were treated with vehicle or 10 μM NO-Cbi for 10 min and ERK (**D**) and Akt (**E**) activation were assessed by blotting with phospho-specific antibodies. Densitometric quantification of pErk and pAkt normalized to total Erk and Akt, respectively, is shown in the bar graphs. **(F)** POBs were serum-starved for 36 h in medium containing 1% BSA with 10 μM NO-Cbi or vehicle; apoptosis was assessed by immunofluorescence staining with antibodies specific for cleaved caspase-3 and FITC-coupled secondary antibodies (green); nuclei were counterstained with Hoechst 33342 (blue). **(G)** POBs were cultured in medium with 0.1% FBS for 18 h, and treated with 10 μM NO-Cbi or vehicle for 1 h; they were transferred to fresh medium containing ^{3}H-thymidine for 24 h, and thymidine incorporation into DNA was measured. (**H,I**) Confluent POBs were differentiated in ascorbate-containing medium for 14 d, with some cells receiving 10 μM NO-Cbi (filled bars) or vehicle (open bars) during the last 24 h. Expression of osteocalcin (OCN), osteopontin (Spp1), collagen 1-A1 (Col1a1), alkaline phosphatase (ALP), low-density

Author Manuscript Author Manuscript Author Manuscript Author Manuscript

lipoprotein receptor-related protein-5 (Lrp5), tubulin (Tuba1), receptor activator of nuclear factor kappa-B ligand (RANKL), and osteoprotegerin (OPG) mRNA was determined by qRT-PCR and normalized to 18S rRNA; normalized mRNA in vehicle-treated cells was assigned a value of 1. Panels A–I show means ± SEM of at least three independent experiments; *$p < 0.05$, **$p < 0.01$, ***$p < 0.001$, for the comparison between NO-Cbi- and vehicle-treated cells. In panel F, $^{\#\#\#}p < 0.01$ for the comparison between cells in starvation *versus* control medium.

Author Manuscript Author Manuscript Author Manuscript Author Manuscript

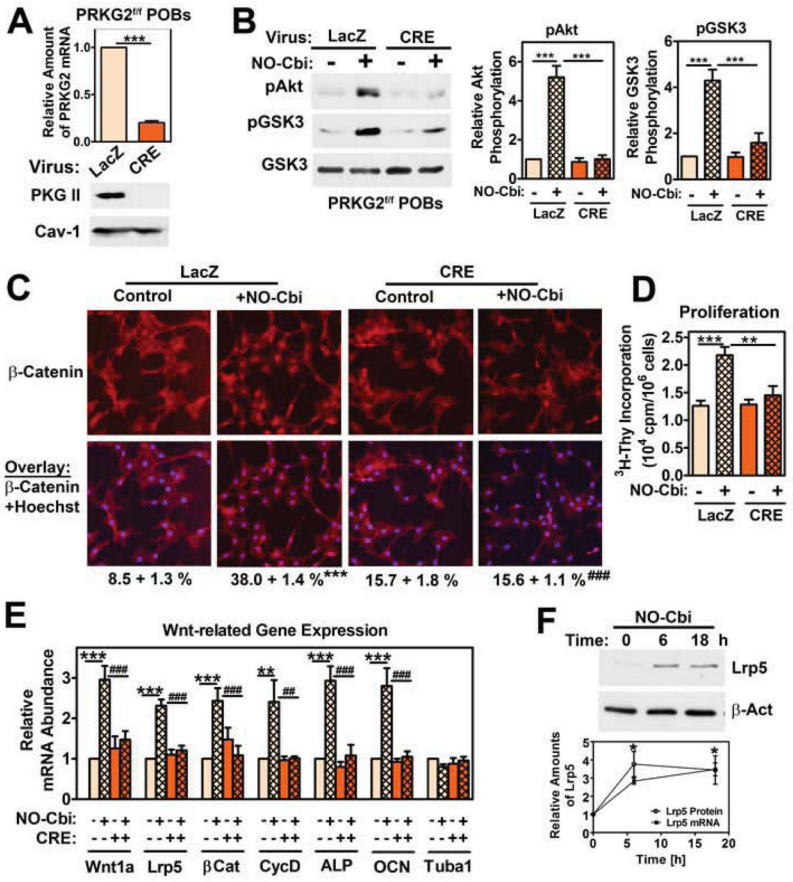

Figure 2. NO-Cbi stimulates Wnt signaling and mPOB proliferation via PKG II

(A) POBs isolated from mice homozygous for *prkg2* alleles flanked by LoxP sites ("floxed" $PRKG2^{f/f}$) were infected with adenovirus expressing β-galactosidase (LacZ, control) or CRE recombinase (CRE). Forty-eight h later, relative amounts of *prkg2* mRNA were determined by qRT-PCR, and knockdown efficiency of PKG II protein was analyzed by Western blotting, with caveolin-1 serving as a loading control. **(B)** Cells were infected as in A, but 30 h later were transferred to medium containing 0.1% FBS, and 18 h later were treated with 10 μM NO-Cbi or vehicle for 10 min. Akt and GSK-3β phosphorylation were assessed using antibodies specific for Akt($pSer^{473}$) and GSK-3β($pSer^{9}$), with total GSK-3β serving as a loading control; densitometric quantification is shown on the right, with relative amounts of pAkt and pGSK-3β found in vehicle-treated, control virus-infected cells assigned a value of 1. **(C)** $PRKG2^{f/f}$ POBs were infected with control or Cre virus and transferred to 0.1% FBS as in B; they were treated with NO-Cbi or vehicle for 6 h, prior to detecting β-catenin by immunofluorescence staining. The bottom panel shows nuclei counterstained with Hoechst 33342. Numbers below indicate the percentage of cells showing nuclear β-catenin. **(D)** Cells were infected and cultured as in B; they were treated with NO-Cbi or vehicle for 1 h prior to measuring ^{3}H-thymidine incorporation into DNA for 24 h. **(E)** Cells were infected with control or CRE virus as described in A, and treated with 10 μM NO-Cbi or vehicle for 24 h. Expression of Wingless type MMTV-integration site family-1a (Wnt1a), low-density lipoprotein receptor- related protein-5 (Lrp5), β-catenin (βCat), cyclin D (CycD), alkaline

Author Manuscript Author Manuscript Author Manuscript Author Manuscript

phosphatase (ALP), osteocalcin (OCN), and tubulin (Tuba1) mRNA was measured by qRT-PCR and normalized to 18S rRNA; normalized mRNA in untreated cells was assigned a value of 1**. (F)** POBs cultured in 10 % FBS were treated with 10 μM NO-Cbi for the indicated times, and Lrp5 protein (open circles) and mRNA (filled squares) were assessed by Western blotting (a representative blot is shown) and qRT-PCR, respectively. Panels A–F show means ± SEM of 3–5 independent experiments in osteoblasts isolated from $PRKG2^{f/f}$ mice in a mixed S129/C57Bl6 background; similar results were obtained in cells from mice back-crossed into the C57Bl6 background (Suppl. Fig. 1). *$p < 0.05$, **$p < 0.01$, ***$p < 0.001$, for the comparison between NO-Cbi-treated *versus* vehicle-treated cells infected with control virus, and $^{\#}p < 0.05$, $^{\#\#}p < 0.01$, $^{\#\#\#}p < 0.001$ for comparison between NO-Cbi-treated cells infected with control *versus* CRE virus.

Author Manuscript Author Manuscript Author Manuscript Author Manuscript

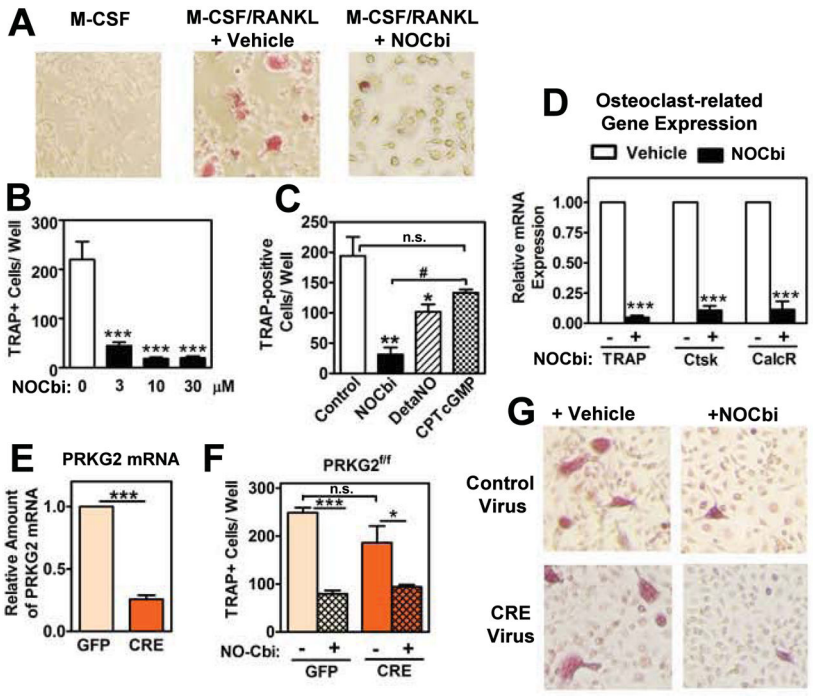

Figure 3. NO-Cbi inhibits osteoclast differentiation

(A,B) Murine bone marrow mono-nuclear cells were cultured in the presence of M-CSF; after 3 d, RANKL was added, with or without NO-Cbi at the indicated concentrations. Tartrate-resistant acid phosphatase (TRAP)-positive cells (red) were counted on day 8. **(C)** Cells were cultured as in A, but some cultures received 10 μM NO-Cbi, 5 μM DETA-NONOate (Deta-NO, which releases two moles of NO per mole of drug), or 100 μM 8-pCPT-cGMP together with RANKL. **(D)** Expression of TRAP, cathepsin K (Ctsk), and calcitonin receptor (CalcR) mRNA was determined by qRT-PCR and normalized to 18S rRNA; normalized mRNA in vehicle-treated cells was assigned a value of 1. **(E–G)** Bone marrow mononuclear cells isolated from PRKG2$^{f/f}$ mice were cultured with M-CSF and RANKL as described in panel A, but 24 h after plating, cells were infected with adenovirus expressing either green fluorescent protein (GFP, control) or CRE. Relative amounts of *prkg2* mRNA were determined by qRT-PCR (E), and TRAP-positive cells were counted on day 8 (F,G). Panels B–F show means ± SEM of at least three independent experiments; *p < 0.05, **p < 0.01, ***p < 0.001, for the comparison between vehicle-treated *versus* drug-treated cells; n.s., non-significant.

Author Manuscript Author Manuscript Author Manuscript Author Manuscript

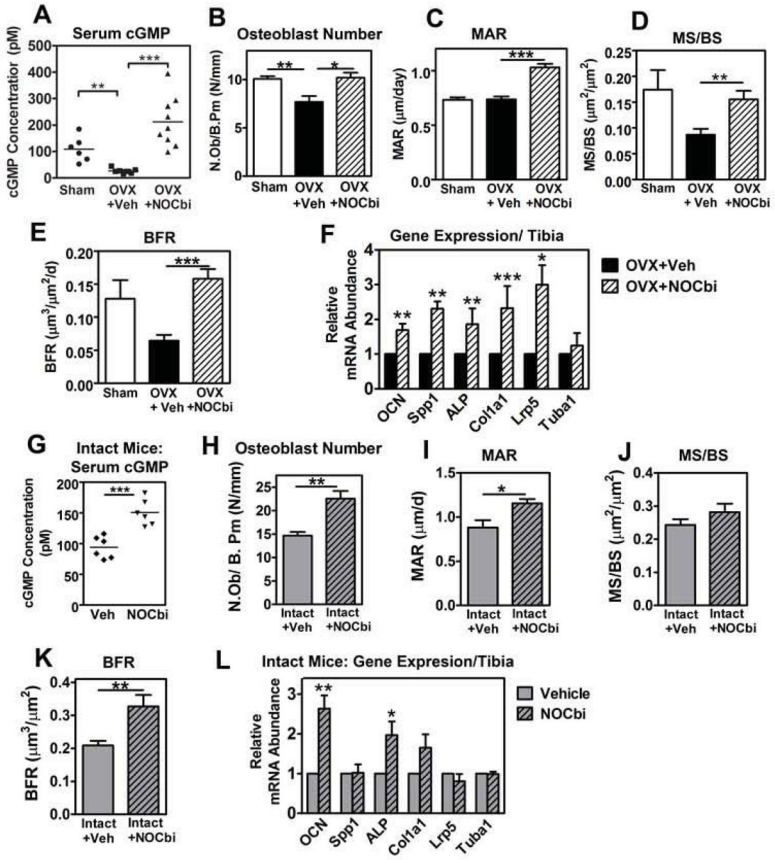

Figure 4. NO-Cbi increases serum cGMP concentration, bone formation, and osteo-blastic gene expression in female mice

(A–F) Eleven week-old mice were subjected to ovariectomy (OVX) or sham operation, and 7 d later daily i.p. injections were started with either vehicle (Veh) or NO-Cbi (10 mg/kg/d) for 6 d per week for 5 weeks. The mice received calcein 7 and 4 d prior to euthanasia. **(G–L)** Twelve week-old intact female mice were randomized to receive vehicle or NO-Cbi and calcein as described for OVX mice. (**A,G)** Serum cGMP concentrations were measured by ELISA 1 h after the last injection of vehicle or NO-Cbi. (**B,H)** The number of trabecular osteoblasts per bone perimeter (N.Ob/B.Pm) was counted at the proximal tibia. **(C–E, I–K)** Trabecular calcein labeling was assessed at the tibia, with quantification of mineral apposition rate (MAR, panels D,I), mineralizing surface per bone surface (MS/BS, panels E,J), and bone formation rate (BFR, panels F,K). **(G,L)** RNA was extracted from femurs, and the relative abundance of osteocalcin (OCN), osteopontin (Spp1), alkaline phosphatase (ALP), collagen-a1 (Col1a1), low-density lipoprotein receptor- related protein-5 (Lrp5) and tubulin (Tuba1) mRNA was quantified by qRT-PCR and normalized to 18S rRNA. Data were calculated according to the ΔΔCT method, using the mean of the vehicle-treated OVX group (F) or the mean of vehicle-treated intact mice (L). Data for panels A–E are the mean ± SEM from n= 6 sham-operated mice, n= 7 vehicle-treated OVX mice, and n=8 NO-Cbi-treated OVX mice; data in panels F–L represent 6 mice per group. *$p < 0.05$, **$p < 0.01$, ***$p < 0.001$ for the indicated pair-wise comparisons.

Author Manuscript Author Manuscript Author Manuscript Author Manuscript

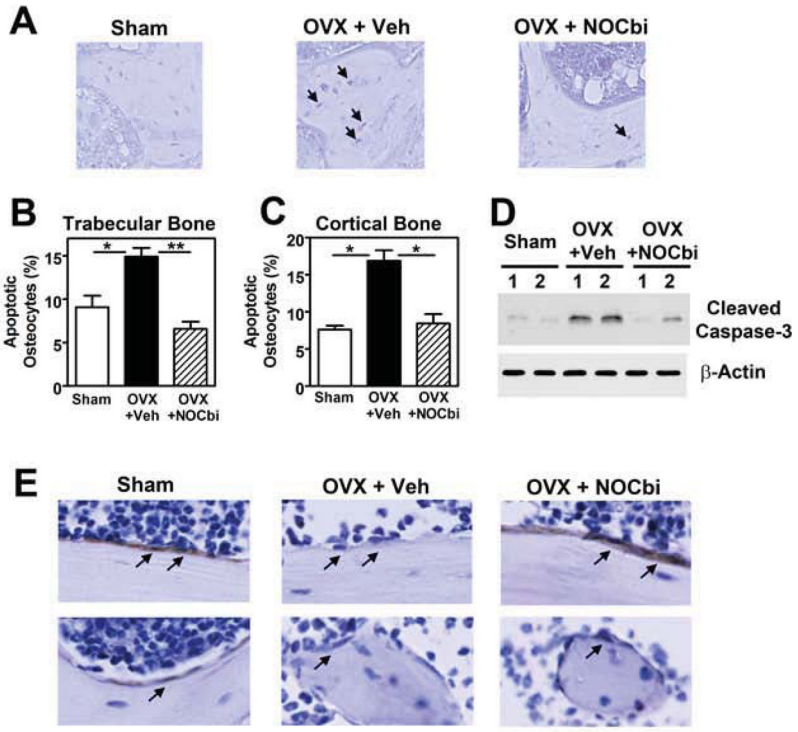

Figure 5. NO-Cbi prevents estrogen deficiency-induced osteocyte apoptosis

Mice were subjected to OVX or sham operation and were treated with vehicle or NO-Cbi as described in Fig. 4. **(A–C)** The percentage of apoptotic osteocytes was assessed in trabecular (A,B) and cortical bone (C) by TUNEL staining (black nuclei) of tibial sections. Data in B and C represent means ± SEM from n= 6 mice per group. *$p < 0.05$, **$p < 0.01$, for the indicated pair-wise comparisons. **(D)** Osteoblast and osteocyte apoptosis was assessed by Western blotting of extracts obtained from tibial bone (after removal of bone marrow), using an antibody specific for cleaved caspase-3, with β-actin serving as a loading control (n =2 mice per group). **(E)** Erk activity in cortical (top) and trabecular (bottom) bone-lining cells was assessed by immunofluorescence staining using a phospho-Erk-specific antibody and horse radish peroxidase-coupled secondary antibody (brown); isotype-matched control IgG produced no signal (not shown).

Author Manuscript Author Manuscript Author Manuscript Author Manuscript

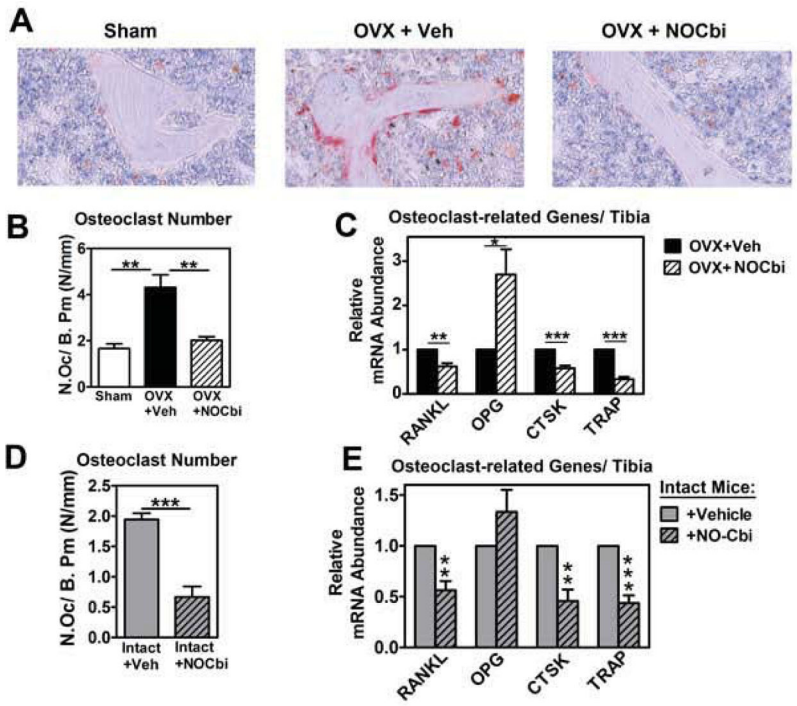

Figure 6. NO-Cbi regulates RANKL/OPG and reduces osteoclasts in female mice

Mice subjected to OVX or sham-operation (A–C) and intact female mice (D,E) were treated with vehicle or NO-Cbi as described in Fig. 4. **(A,B, D)** Osteoclasts were identified by TRAP staining (red), and the number of trabecular osteoclasts per bone perimeter (N.Oc/B.Pm) was counted at the proximal tibia. **(C,E)** RNA was extracted from femurs, and the relative abundance of RANKL, OPG, CTSK, and TRAP mRNA was quantified by qRT-PCR and normalized to 18S rRNA. Data were calculated according to the ΔΔCT method using the mean of the vehicle-treated OVX group (C), or the mean of vehicle-treated intact mice (E). Data represent the mean ± SEM from 6 mice per group. *$p < 0.05$, **$p < 0.01$, ***$p < 0.001$ for the indicated pair-wise comparisons.

Author Manuscript Author Manuscript Author Manuscript Author Manuscript

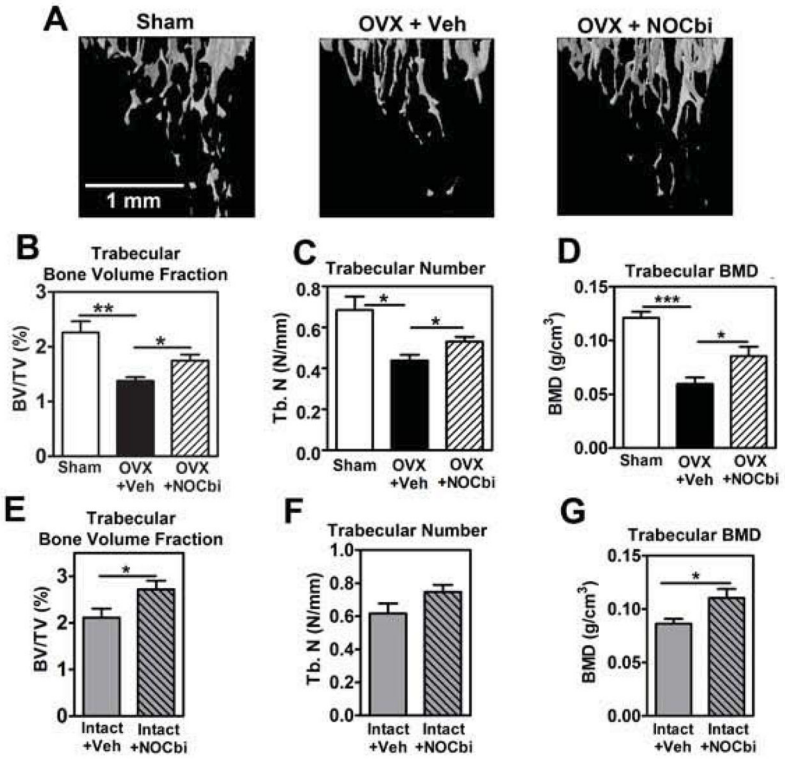

Figure 7. NO-Cbi increases trabecular bone mass in female mice

Mice subjected to OVX or sham operation (A–D) and intact female mice (E–G) were treated with vehicle or NO-Cbi as described in Fig. 4. (**A**) Tibiae were analyzed by micro-CT imaging, and three-dimensional reconstruction of the trabecular bone at the proximal tibia below the growth plate is shown. (**B–G**) Trabecular bone volume/tissue volume (B,E), trabecular number (C,F), and trabecular bone mineral density (D,G) were quantified at the proximal tibia as described in Materials and Methods. Data in panels B–D represent means ± SEM from n= 6 sham-operated mice, n= 7 vehicle-treated OVX mice, and n=8 NO-Cbi-treated OVX mice; data in panels E–G are from 6 intact female mice per group. *p < 0.05, **p < 0.01, ***p < 0.001 for the indicated pair-wise comparisons.